# FLUX AND ENERGY SPECTRUM OF COSMIC RAY ELECTRONS BETWEEN 10 AND 1000 GeV

Peter Meyer and Dietrich Müller
Enrico Fermi Institute and Department of Physics
University of Chicago, Chicago, Illinois U.S.A.

A balloon borne counter-detector with a geometry factor of 0.1 $m^2$ ster has been exposed for a total of 64 hours under about 4.6 $g/cm^2$ of residual atmosphere above Palestine, Texas in 1970. The experimental technique and the method of data analysis is described, and preliminary results of this investigation, based on about 45% of the total amount of available data, are presented. The resulting electron flux is slightly lower than that reported by Anand et al. (1970) and can, over the entire energy range, be represented by a power law with spectral index of about -2.8.

1. Introduction. The shape of the energy spectrum of cosmic ray electrons of energies beyond 100 GeV is closely related to the electro-magnetic conditions in interstellar space and to the lifetime and source distribution of cosmic rays in the galaxy. A number of investigations have therefore been carried out, using nuclear emulsion as well as counter techniques to study the shape of the electron spectrum at high energies (Anand et al. 1968, 1970; Nishimura et al. 1970; Scheepmaker and Tanaka 1971; Marar et al. 1971; Fanselow et al. 1971). Unfortunately, the agreement of the published data is rather poor, leading to discrepancies of roughly an order of magnitude in the 100 GeV region. These discrepancies seem to be caused by the low flux of electrons, the difficulty of discrimination against proton induced events, and the absence of laboratory calibrations beyond 20 GeV. While emulsion detectors should, in principal, allow for a unique distinction between proton- and electron events, these detectors become impractical if large geometric factors are required. Therefore, we have designed a large size counter-detector which uses extensive pulse height analysis, time of flight analysis, and statistical methods to identify electron events.

2. Description of the Experiment. Fig. 1 shows a schematic cross-section of the detector. Its main elements are: (a) a telescope of plastic scintillation counters T1, T3, yielding a geometry factor of about 1000 $cm^2$ ster. (b) a directional gas Cerenkov counter T2 (1 atm. Freon 12) to discriminate against

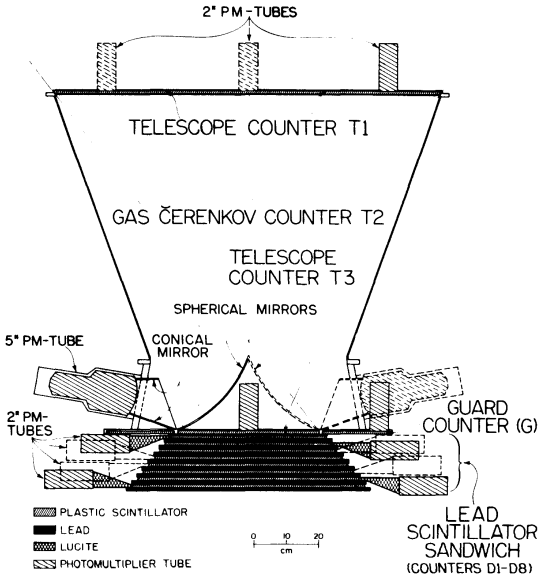


Fig. 1. Schematic cross-section of the detector system. The counter arrangement is rotationally symmetric around the vertical axis.

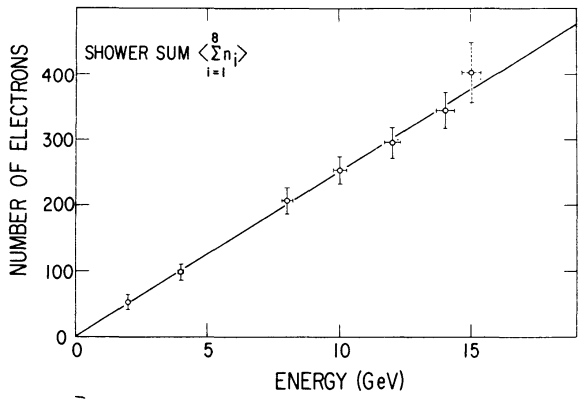


Fig. 2. The average shower sum vs. energy of incident electrons from accelerator.

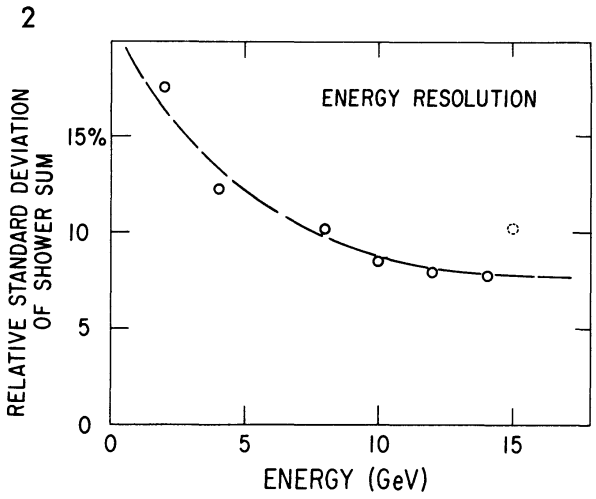


Fig. 3. The relative standard deviation of the shower sum vs. energy, displaying the energy resolution of the instrument.

protons of less than about 20 GeV and against particles traversing the instrument from below. (c) a lead-scintillator sandwich of 18.5 radiation lengths of lead, which acts as a shower detector. Eight plastic scintillators D1...D8 are spaced by 2.5 r.l. of lead each, 1 r.l. is in front of D1. (d) a ring shaped guard counter G to obtain additional information on particles entering the instrument from the side. All counters except T2 are pulse height analyzed (256 channels with quasi logarithmic response). To accept an event, a fast coincidence T1, T2, T3, D6 is required. To obtain independent information on the direction of incoming particles, for each event the time of flight between T1 and T3 is measured.

The instrument has been calibrated at SLAC with electrons and pions of 2 to 15 GeV energy. As expected, the sum of the signals of the counters D1...D8 (in the following called shower sum) is proportional to the energy of incident electrons. This is shown in Fig. 2, where the average shower sum is plotted vs. energy. Fig. 3 shows the relative standard deviation of the shower sum, indicating the energy resolution of the instrument. The average shower profiles as measured at SLAC for electrons, as well as profiles which are extrapolated to higher energies, using predictions of the analytical shower theories are plotted in Fig. 4.

This instrument has been exposed in three balloon flights from Palestine, Texas (geomagnetic cut-off 4.5 GV) during 1970, for a total of 64 hours under about 4.6 g/cm$^2$ of residual atmosphere. In flight calibration has been provided by penetrating $\alpha$-particles.

3. Data Analysis. At this writing, we have analyzed about 45% of the total acquired data. As expected, the majority of the recorded events is not due to electrons. While most of the background events can be readily identified due to their off "shower" profiles, a considerable number of predominantly proton induced events may masquerade as electrons. As demonstrated in Fig. 5, the time-of-flight analyzer turned out to be extremely useful in order to discriminate against unwanted events. About 50% of the events seem to trigger counter T3 prior to triggering T1. These events are probably caused by particles entering the detector from the side and producing a large number of secondary particles.

The data analysis was handled in the following sequence: First, the shower sum for each event (sum of the 8 signals $n_{im}$ of D1 to D8) was determined. Thereby, for each event an effective energy E is obtained. E is the energy an "ideal" electron would have in order to produce the same shower sum. Then the measured pulse height profile $n_{im}$ (i = 1...8) is compared with the expected profile $n_{ie}$ of the corresponding electron shower by means of a goodness of fit parameter Q, where

$$Q = \frac{1}{8} \sum_{i=1}^{8} [ (n_{im} - n_{ie})^2 / \sigma_i^2 ]$$

($\sigma_i$ are the expected standard deviations of $n_{ie}$, their values are extrapolated from the SLAC data). Further, the "starting point" of each event is determined. Electron showers start to develop within the first radiation length of lead with very high probability, while showers due to interacting protons may start with almost equal probability anywhere in the lead-sandwich. As illustrated in Fig. 6, we have compared each event with a series of 8 electron shower profiles, which correspond to the same energy E, but whose starting points are shifted in steps of 0.5 r.l. into the lead. The shower profile to which an event fits best (smallest $Q = Q_{min}$) defines, therefore, the starting point of that event. Fig. 7 shows typical starting point distributions for electrons (from SLAC, the shape of this distribution is practically independent of the primary energy), for interacting pions (from SLAC, the pile-up at 3.5 r.l. is due to pions which interact at a greater depth), and events observed in flight. If the flight events are mainly electrons and interacting protons, and if protons and pions behave similarly, we may interpret the

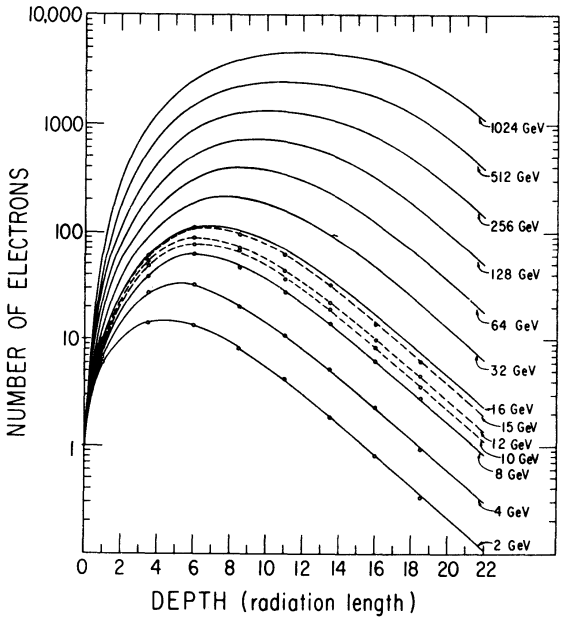


Fig. 4. Average shower profiles obtained with electrons from the SLAC accelerator and extrapolated shower profiles toward higher energies.

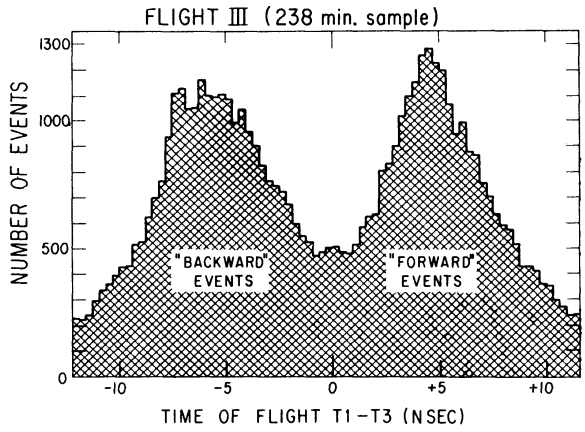


Fig. 5. Time of flight between counters T1 and T3, showing that about 50% of the events originate from interactions in the lead stack without first triggering counter T1.

starting point distribution of the flight events as a superposition of the sharply peaked electron distribution and the rather flat pion distribution and may, thereby, determine the number of electrons in this sample of data. However, in order to obtain meaningful results by this method, we have first to exclude all events which are obviously not electron-like: backwards moving particles, events which do not fit reasonably well to any of the shifted shower profiles ( $Q_{min} > 10$), and events for which the signals in T3 and G are excessively large.

4. Results. The differential electron spectrum as obtained by this method is shown in Fig. 8. For comparison, we also show some recently published data which are obtained by means of emulsion techniques (Anand et al., 1970, Nishimura et al., 1970) (open symbols) and with counter detectors (Scheepmaker and Tanaka, 1971; P. Schmidt 1971, Fanselow et al. 1971) (solid symbols). The accuracy of our data is not limited by statistics. Rather, the vertical error bars indicate the uncertainty in our method of background reduction at the present status of the analysis. Also, the arrow-like symbols at the high energy end should not indicate that these points are upper limits, but that we believe that the actual flux is more likely near the lower end of the vertical bars.

5. Discussion. Our measurement seems to indicate slightly lower electron fluxes than the average of other experiments, and in particular, lower fluxes than those from other counter-experiments. Over the whole energy range, the data points can be reasonably well fitted by a power law of spectral index -2.8 ± 0.1. At the present status of our analysis, a break in the slope of the electron spectrum is not noticeable. To further reduce the error in our data we plan to recalibrate the instrument with high energy protons in order to understand better the shape of pulse height profiles due to interacting protons. Nevertheless, if the absence of a steepening in the electron spectrum up to almost 1000 GeV should be further

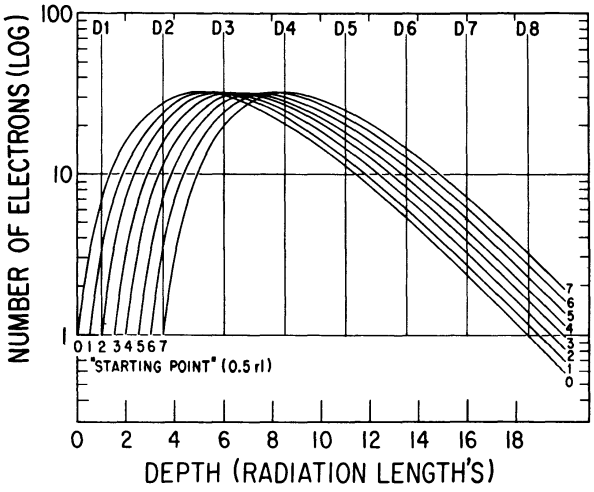


Fig. 6. Typical shower profiles with starting points at various depths in the lead stack.

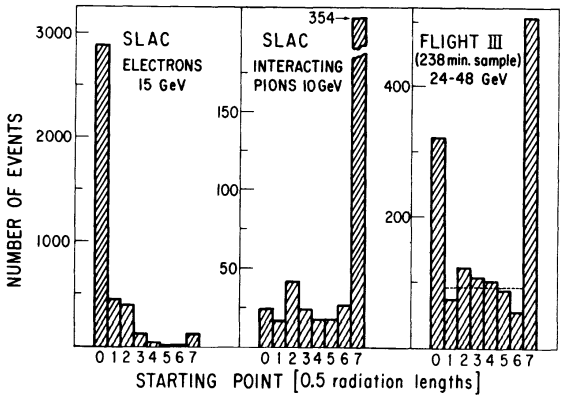


Fig. 7. Observed starting point distributions for showers produced by electrons and pions from the SLAC accelerator and from a sample of flight data.

substantiated, it will be necessary to modify the presently accepted ideas about the propagation and lifetime of cosmic ray electrons in the galaxy. Either the electron lifetime will be significantly less than $10^6$ years, or the energy density of the interstellar magnetic and photon fields will have to be reduced below presently accepted values. However, we wish to postpone speculations about these consequences until after our data analysis is completed.

For their contributions to this work we express our thanks to E. Juliusson, V. T. Kurtz, G. Kelderhouse, D. Hunsinger, W. Hollis, W. Johnson and Mrs. H. Shaw. We greatly appreciate the support given to us by the staff of SLAC for calibration runs, and the staff of the NCAR balloon facility for three excellent flights. This work was supported in part by the National Aeronautics and Space Administration under Grant NGL 14-001-005.

References.

Anand, K. C., Daniel, R. R., Stephens, S. A., 1968. Phys. Rev. Letters 20, 764.

Anand, K. C., Daniel, R. R., Stephens, S. A., 1970. Acta Phys. Hung. 29, Suppl. 1, 229.

Fanselow, J. L., Hartman, R. C., Meyer, P. and Schmidt, P. J., 1971. Astrophys. and Space Sci. (in press).

Marar, T. M. K., Freier, P. S., and Waddington, C. J., 1971. J. Geophys. Res. 76, 1625.

Scheepmaker, A. and Tanaka, Y., 1971. Astronomy and Astrophysics, 11, 53.

Schmidt, P., 1971. (to be published).

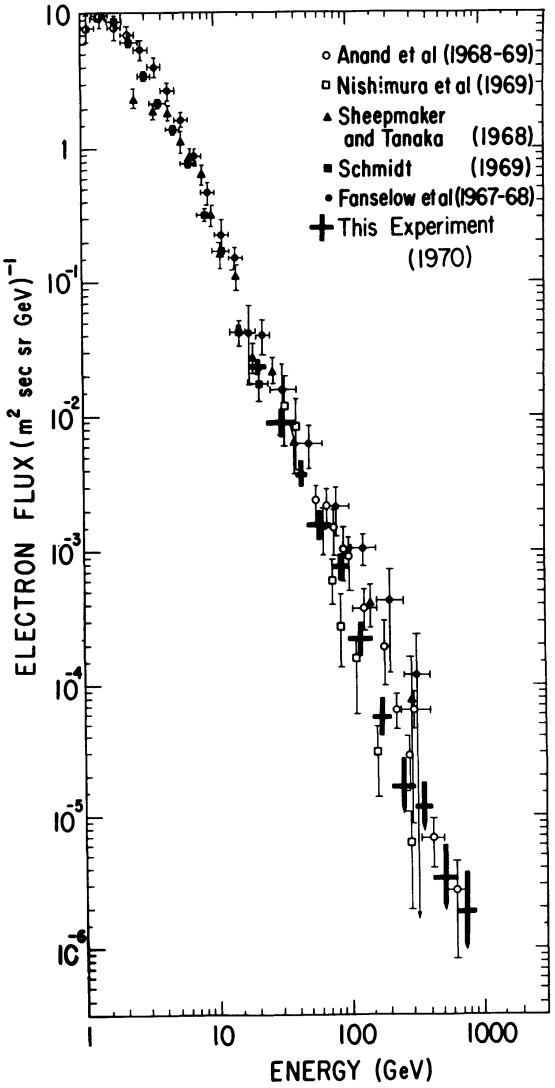


Fig. 8. The primary electron energy spectrum measured in this experiment compared with results by other authors.